BMC Oral Health

RESEARCH

Open Access

Evaluation of cuspid cortical anchorage with different sagittal patterns using cone-beam computed tomography: a retrospective study

Xiaoyu Wei[1,2], Yaqi Lin[2], Guanning Zhang[1,2], Jiawen Zheng[1,2], Lanxin Zhang[1,2], Yuqing Yang[1,2] and Qing Zhao[1,2*]

Abstract

Background No studies have focused on cortical anchorage resistance in cuspids, this study aimed to characterize the cortical anchorage according to sagittal skeletal classes using cone-beam computed tomography (CBCT).

Methods CBCT images of 104 men and 104 women were divided into skeletal class I, II, and III malocclusion groups. Skeletal and dental evaluations were performed on the sagittal and axial cross-sections. One-way analysis of variance followed by least significant difference post-hoc tests was used for group differences. Multiple linear regression was performed to evaluate the relationship between influential factors and cuspid cortical anchorage.

Results All cuspids were close to the labial bone cortex in different sagittal skeletal patterns and had different inclinations. There was a significant difference in the apical root position of cuspids in the alveolar bone; however, no significant difference in the middle or cervical portions of the root was found between different sagittal facial patterns. The middle of the cuspid root was embedded to the greatest extent in the labial bone cortex, with no significant difference between the sagittal patterns. For all sagittal patterns, 6.03 ± 4.41° (men) and 6.08 ± 4.45° (women) may be appropriate root control angles to keep maxillary cuspids' roots detached from the labial bone cortex.

Conclusions Comparison of skeletal class I, II, and III malocclusion patients showed that dental compensation alleviated sagittal skeletal discrepancies in the cuspid positions of all patients, regardless of the malocclusion class. Detailed treatment procedures and clear treatment boundaries of cuspids with different skeletal patterns can improve the treatment time, periodontal bone remodeling, and post-treatment long-term stability. Future studies on cuspids with different dentofacial patterns and considering cuspid morphology and periodontal condition may provide more evidence for clinical treatment.

Keywords Three-dimensional imaging, Cone-beam computed tomography, Alveolar bone, Cuspids, Skeletal malocclusion, Orthodontic treatment

*Correspondence:
Qing Zhao
fanfan_qing@163.com

[1]Orthodontic Centre, West China College of Stomatology, Sichuan University, 14#, 3rd Section, Renmin South Road, Chengdu 610041, China
[2]State Key Laboratory of Oral Diseases, Sichuan University, 14#, 3rd Section, Renmin South Road, Chengdu 610041, China

© The Author(s) 2023. **Open Access** This article is licensed under a Creative Commons Attribution 4.0 International License, which permits use, sharing, adaptation, distribution and reproduction in any medium or format, as long as you give appropriate credit to the original author(s) and the source, provide a link to the Creative Commons licence, and indicate if changes were made. The images or other third party material in this article are included in the article's Creative Commons licence, unless indicated otherwise in a credit line to the material. If material is not included in the article's Creative Commons licence and your intended use is not permitted by statutory regulation or exceeds the permitted use, you will need to obtain permission directly from the copyright holder. To view a copy of this licence, visit http://creativecommons.org/licenses/by/4.0/. The Creative Commons Public Domain Dedication waiver (http://creativecommons.org/publicdomain/zero/1.0/) applies to the data made available in this article, unless otherwise stated in a credit line to the data.

Background

Orthodontics is dedicated to the precise control of tooth position in a three-dimensional (3D) orientation to achieve an ideal occlusal relationship with targeted tooth movement. This has led to the emergence of edgewise orthodontic systems, straight-arch orthodontic systems, and aligners [1, 2]. However, the evolution of orthodontic systems and materials has not fundamentally altered the orthodontic treatment philosophy of aligning the teeth, closing the extraction space under the 3D control of the teeth, and refining the occlusal relationship.

In clinical practice, anterior tooth intrusion and cuspid distal movement with either fixed orthodontic appliance systems or clear aligner systems are often difficult. Orthodontic tooth movement involves bone remodeling, with bone resorption on the pressure side and bone formation on the tension side, and is influenced by factors, such as the orthodontic force, bone density, and cortical anchorage [3, 4]. One of the key factors is the proximity of the tooth root to the cortical bone. In contrast to the porous structure of the cribriform plate and the less dense cancellous bone, the thin, hard layer of bone cortex provides sufficient resistance to tooth movement [5], and the bone cortex is often distributed in the direction of expected tooth movement, such as the labial bone cortex during intrusion of the anterior teeth, and the buccolingual bone cortex in the extraction area during closure of the extraction space. Appropriate torque settings are critical to avoid cortical anchorage. As the roots are generally submerged in the alveolar bone and invisible within the oral cavity, the tooth torque is often set based on visual inspection or experience, which may cause cortical anchorage and impede smooth and physiological orthodontic treatment.

To study the limits of tooth movement, some studies have focused on the thickness of the alveolar bone or the bone cortex [6, 7]. Additionally, studies have reported modulating alveolar bone remodeling in the incisal region after orthodontic treatment to overcome the limitations of orthodontic tooth movement [8]. Most patients with malocclusion have skeletal discrepancies, and the linked compensations of alveolar bone morphology and tooth angles increase the difficulty of diagnosis [9]. Moreover, different sagittal skeletal patterns are associated with different degrees of risk of dehiscence and fenestration [10]. Recent studies have therefore focused on the effect of different skeletal facial morphologies on the thickness of the alveolar bone in the anterior region or on the position of the anterior teeth in the alveolar bone [11–13]. However, most studies did not consider the cortical and cancellous bone separately and have focused on the incisors. The cuspids, unlike the incisors, have the longest and thickest roots, are located at the turn of the arch, and are subject to both sagittal and transverse orientation influences. Thus, the torque of the cuspids cannot be accurately determined by intraoral observation and two-dimensional (2D) panoramic radiography alone [14]. Cuspid cortical anchorage, a crucial factor in the alignment and closure of the extraction space, has rarely been studied. Identifying the inclination and position of the cuspids facilitates their physiological movement and avoidance of iatrogenic dehiscence or fenestration.

Cone-beam computed tomography (CBCT) has been widely used in dentistry because it provides more comprehensive information relative to 2D images [15]. To our knowledge, no study has demonstrated the position of cuspids in relation to the alveolar bone and the method of cuspid compensation in different sagittal skeletal patterns using 3D images. Therefore, this study aimed to analyze the characteristics of cuspid roots cortical anchorage in patients with different sagittal skeletal facial morphologies using CBCT, evaluate the potential skeletal and dental features that may influence the relationship between cuspid root and alveolar bone cortex, and investigate the relatively ideal root control angle that should be applied when the cuspids are detached from the bone cortex to provide a reference for orthodontists to set the cuspid position.

Methods

This retrospective cross-sectional study was approved by the Ethics Committee of the National Key Laboratory of Oral Diseases and the Ethics Committee of the West China Stomatology Hospital of Sichuan University (protocol number: WCHSIRB-D-2020-399). The study sample was selected from patients who visited. We searched the hospital case system to screen for cases with CBCT examinations in the primary diagnosis data and collected participants according to the following inclusion and exclusion criteria. CBCT is performed at the discretion of the treating physician and is used to provide information that is insufficient to provide with 2D images of the temporomandibular joint, roots, and obstructed teeth, etc. We explained the purpose of our study in detail to the participants, and all participants understood and signed informed consent.

The inclusion criteria were as follows: (1) facial symmetry; (2) complete permanent dentition; (3) no posterior crossbite or scissors bite; (4) well-aligned maxillary and mandibular anterior teeth with fully developed cuspid roots and no significant root curvature (The severity of crowding is less than 2 mm); (5) no bone defects: the distance from the top of the alveolar ridge to the cementoenamel junction (CEJ) of the cuspid should be less than 3 mm [16]; and (6) normodivergent facial patterns (22° ≤ Frankfort mandibular plane angle (FMA) ≤ 30°). The exclusion criteria were as follows: (1) history of orthodontic treatment; (2) pathological changes, such as

periapical inflammation, cysts, tumors, and root resorption involving the cuspid region; and (3) systemic diseases. After screening, 208 patients (104 men and 104 women; 25.42±6.24 years), with randomly selected unilateral 208 maxillary cuspids, were included in this study and divided into three groups according to the degree of ANB angle (The intersection angle of the line connecting the subspinale, nasion and supramental points) on cephalometric findings: skeletal class I malocclusion (n=64, ANB angle between 1° and 4° and an angle class I molar relationship), skeletal class II malocclusion (n=78, ANB angle greater than 4° and an angle class II molar relationship), and skeletal class III malocclusion (n=66, ANB angle less than 1° and an angle class III molar relationship); the demographic data are shown in Table 1. The sample size was calculated based on a previous study using PASS software (version 15; Kaysville, Utah, USA) with 80% power of test and 0.05 significance level as reference [17].

All CBCT data were obtained using a CBCT machine (3D Accuitomo F170; J Morita Manufacturing, Kyoto, Japan) with exposure parameters of 4.5 mA and 85 kV, exposure time of 17.5 s, voxel size of 0.25 mm, and scan area of 140×100 mm. All digital lateral cephalometric were obtained by the same radiographer (Vatech PaX-I 2D, Gyeonggi, Korea). One investigator randomly numbered all CBCT and cephalometric data without patient information. The data were measured by two other investigators using Dolphin Imaging Software (version 11.9 premium, Dolphin Imaging & Management Solutions, Chatsworth, USA) and i-Dixel One Volume Viewer software (i-Dixel 3DX, Version 2.8, J Morita Mfg. Corp., Osaka, Japan).

The 3D spatial position of the cuspids was represented by three mutually perpendicular planes and the reconstructed image in the i-Dixel software (Fig. 1). All measurements were performed in the maximal labiolingual direction of each tooth, a method validated in previous studies [18]. As shown in Fig. 2, the green guideline crossed the maximum labial-palatal diameter of the cuspid in the axial plane, and the green and blue guidelines passed through the cusp and apical points of the cuspid in the coronal and sagittal planes, separately. A_1, the mid root point (A_2), and a point 4 mm below the CEJ (A_3) helped determine the three measurement planes L_1, L_2, and L_3 (Fig. 3). The alveolar bone midpoints (Q_1 and Q_3) in the L_1 and L_3 sections were connected to determine the direction of the alveolar bone inclination, and the cuspid inclination angle (α) was the angle at which the alveolar bone inclination line and long axis of the cuspid intersected (Fig. 4). The cuspid and alveolar landmarks in the axial plane at three levels are illustrated in Fig. 5. The center points of the pulp chambers of the maxillary and mandibular left and right cuspids were used to measure the maxillary and mandibular intercuspid alveolar bone width (W-upper and W-lower) (Fig. 6). To calculate the rotation angle (β) of the cuspid detached from the labial bone cortex with D as the center of rotation, the radius of rotation $r = M_2\text{-}D = ((A_2\text{-}D)^{2} + (A_2\text{-}M_2)^{2})^{1/2}$ was calculated using the Pythagorean theorem. According to the arc length formula, arc $l = 2\pi r \times \beta/360$. Given that l is much smaller than the radius r, for simplicity of calculation, l was set to approximately $M_2\text{-}IB_2$, and then $\beta \approx (M_2\text{-}IB_2) \times 360 / 2\pi r$ (Fig. 7). All CBCT measurement data were analyzed using a scale with an accuracy level of 0.01 mm. The cuspid, alveolar, and measuring plane landmarks are defined in Table 2, and all measurements are presented in Table 3. The value was negative if the cuspid root landmarks were farther from the center of the alveolar bone than the alveolar bone landmarks.

Before the measurements, two investigators were trained by a professor of orthodontics and a professor of radiology with extensive experience to improve the measurement accuracy. Then, 20% of the cephalometric lateral radiographs and CBCT data were randomly selected, and each investigator measured the data twice, with a one-week interval between each measurement. Intragroup and intergroup correlation coefficient analyses were used to test the intraobserver and interobserver consistency. Normality tests were performed using the Shapiro-Wilk test. One-way analysis of variance followed by least significant difference post-hoc tests was used to compare the differences between different group measures. Skeletal and dental characteristics including ANB, FMA, U1-SN (Posterior inferior intersection angle between the long axis of the upper central incisor and the SN plane), W-upper, W-lower, WUL and α were selected in stepwise multiple linear regression, which was conducted to assess potential characteristics that may have an effect on $A_1\text{-}IB_1$, $M_2\text{-}IB_2$ and $M_3\text{-}IB_3$. All statistical analyses were conducted using IBM SPSS Statistics

Table 1 Demographic data of the subjects

	Class I		Class II		Class III	
	Men	Women	Men	Women	Men	Women
n	32	16	38	20	34	16
Age(y)	24.97±5.72	26.84±6.54	26.03±7.68	26.98±7.86	23.71±3.15	23.63±3.62
ANB(°)	2.38±0.76	2.48±0.76	6.29±1.72	5.52±1.25	−2.90±3.28	2.00±2.05
FMA(°)	24.66±2.35	24.37±2.06	24.75±2.08	24.7±2.10	23.85±2.07	23.80±1.18

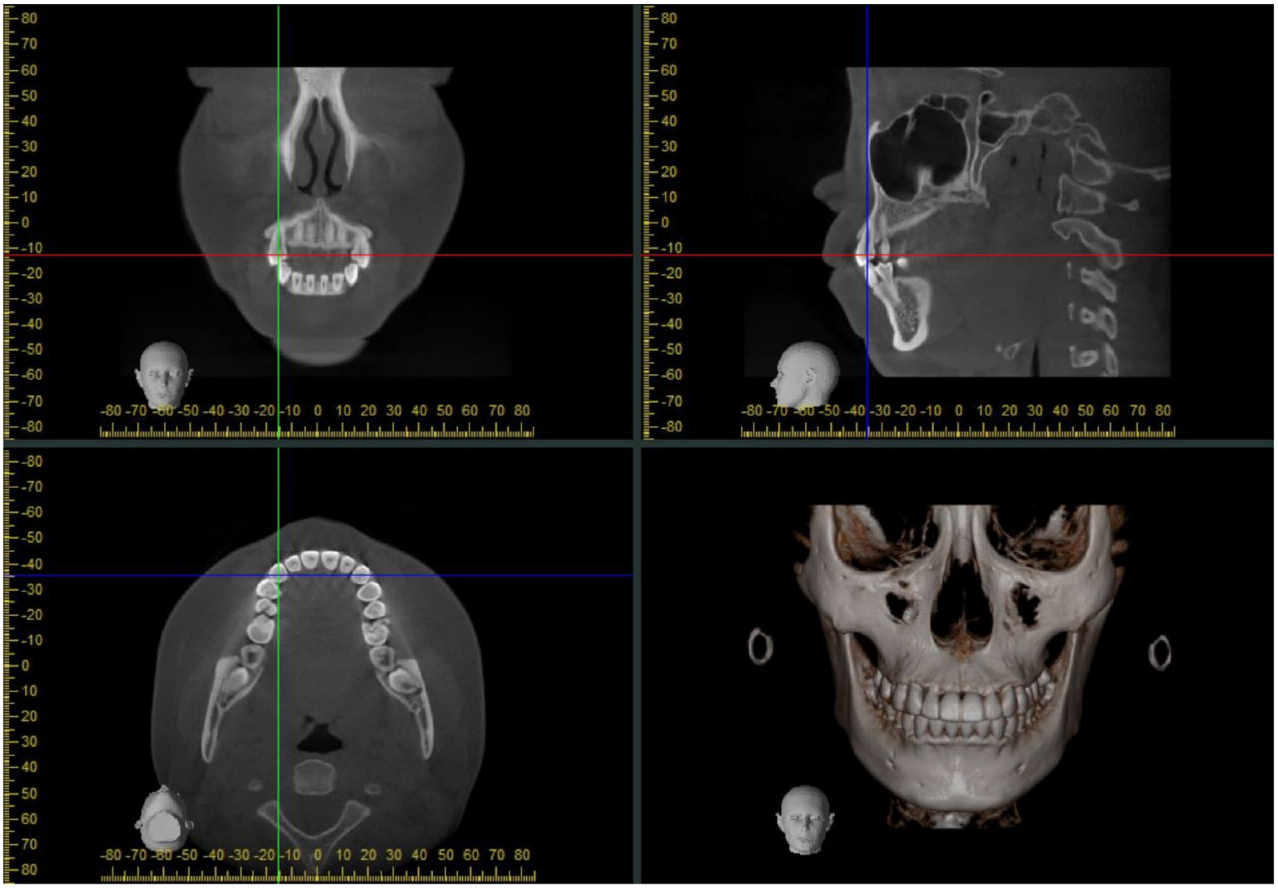

Fig. 1 Three-dimensional image presentation of CBCT. The green guideline adjusts the sagittal orientation. The red guideline adjusts the axial orientation. The blue guideline adjusts the coronal orientation

for Windows (Version 26.0; IBM Corporation, Armonk, New, USA). Statistical significance was set at $P<0.05$.

Results

In this study, the intergroup and intragroup coefficients of all variables are greater than 0.95, which show excellent intergroup and intragroup reproducibility of the measurements.

Table 4 shows the alveolar bone thickness and labial and lingual bone cortical thickness at apical, middle, and cervical root levels in patients with skeletal class I, class II, and class III malocclusion. There were no significant differences between the three malocclusion classes.

Table 5 shows the position of the cuspid roots relative to the alveolar bone in the different skeletal facial types. At the apical root level, cuspid roots were close to the labial bone cortex in both sexes in class II. The apical portion of the roots was farther away from the labial bone cortex in skeletal class I of women and class III of men malocclusion than in class II of both sexes, with significant difference. At the middle and cervical root levels, there were no significant differences in the position of the cuspid roots in any of the groups. However, it should be noted that at the middle root level, the roots of the cuspids touched the labial bone cortex and were close to the outer edge of the labial bone cortex. At the cervical root level, the roots of the cuspids still touched the labial bone cortex.

Table 6 compares the position of the cuspid roots relative to the labial bone cortex at different levels in patients with the same malocclusion type. The roots of the cuspids at the middle root level were located to the greatest extent in the labial bone cortex for all skeletal malocclusion types.

Table 7 shows no significant difference in root length and ideal root control angle among the different class groups. The mean ideal root control angle was $6.03\pm4.41^{\circ}$ in men and $6.08\pm4.45^{\circ}$ in women.

Table 8 demonstrates the factors influencing the cortical anchorage of cuspids by stepwise multiple linear regression. In general, cross-sectional indicators including W-lower and WUL; vertical indicators including FMA; and sagittal indicators including U_1-SN and ANB all had an effect on the cortical anchorage of the cuspids. Only α, an indicator related to both cross-sectional and

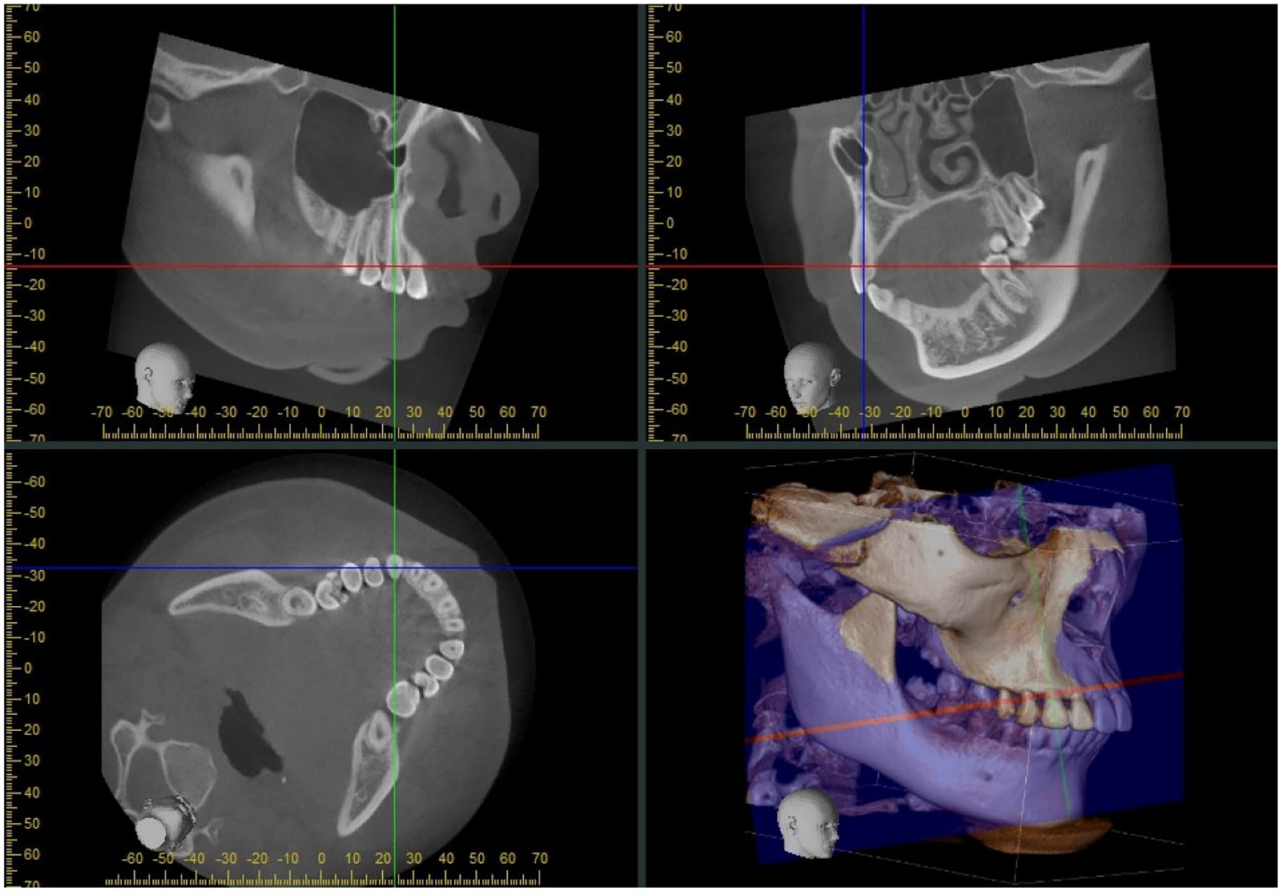

Fig. 2 Presentation of the reference planes for the measurement of the cuspid

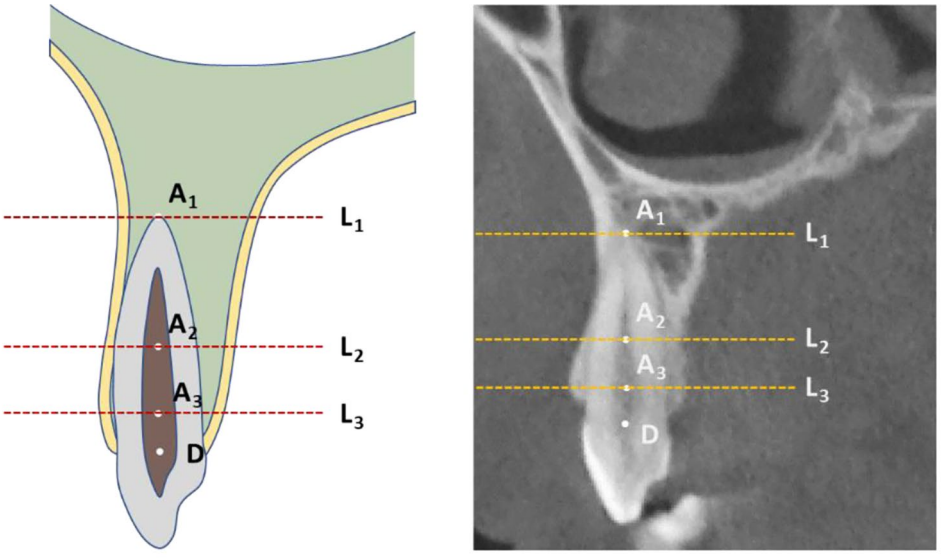

Fig. 3 Three levels of the cuspid root. A_1: the apical point of the cuspid; A_2: the mid-root point of the cuspid; A_3: the cervical-root of the cuspid; D: the intersection of the long axis of the cuspid and the CEJ; L_1: the apical-root level; L_2: the mid-root level; and L_3: the cervical-root level

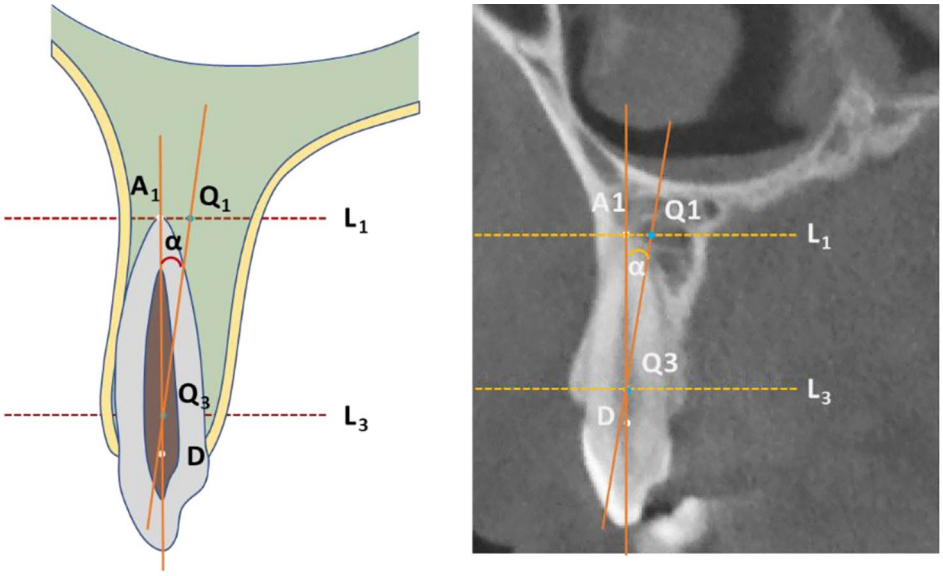

Fig. 4 Inclination angle of the cuspid. Q_1: the alveolar bone midpoint at the L_1 level; Q_3: the alveolar bone midpoint at the L_3 level; and α: the inclination angle of the cuspid

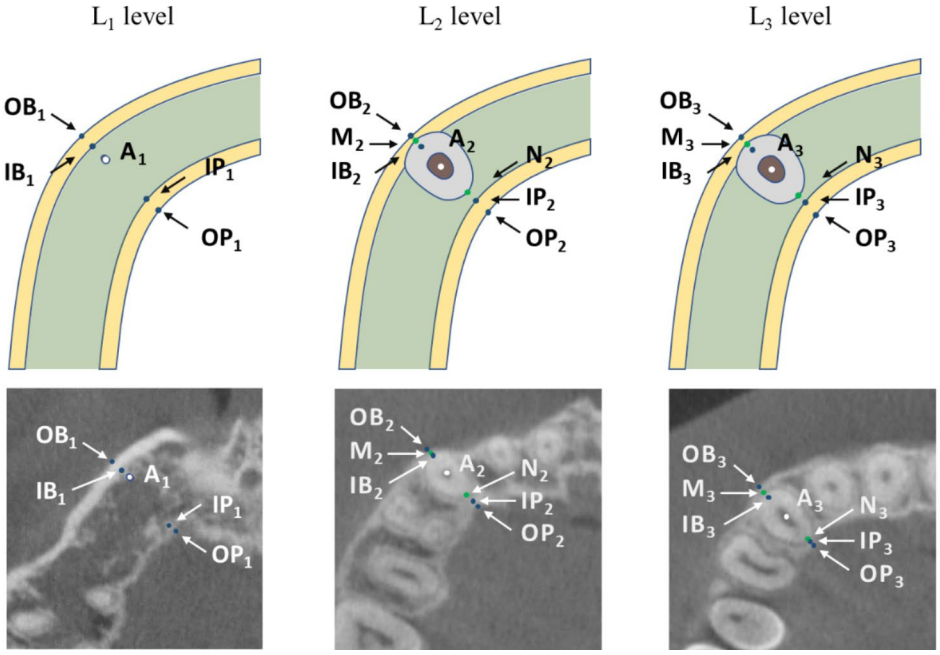

Fig. 5 Marking points of the root and the alveolar. OB_1: the outer edge of the labial bone cortex at the L_1 level; IB_1: the inner edge of the labial bone cortex at the L_1 level; IP_1: the inner edge of the palatal bone cortex at the L_1 level; OP_1: the outer edge of the palatal bone cortex at the L_1 level; OB_2: the outer edge of the labial bone cortex at the L_2 level; IB_2: the inner edge of the labial bone cortex at the L_2 level; IP_2: the inner edge of the palatal bone cortex at the L_2 level; OP_2: the outer edge of the palatal bone cortex at the L_2 level; M_2: the labial tangent point of the root at the L_2 level; N_2: the palatal tangent point of the root at the L_2 level; OB_3: the outer edge of the labial bone cortex at the L_3 level; IB_3: the inner edge of the labial bone cortex at the L_3 level; IP_3: the inner edge of the palatal bone cortex at the L_3 level; OP_3: the outer edge of the palatal bone cortex at the L_3 level; M_3: the labial tangent point of the root at the L_3 level; and N_3: the palatal tangent point of the root at the L_3 level

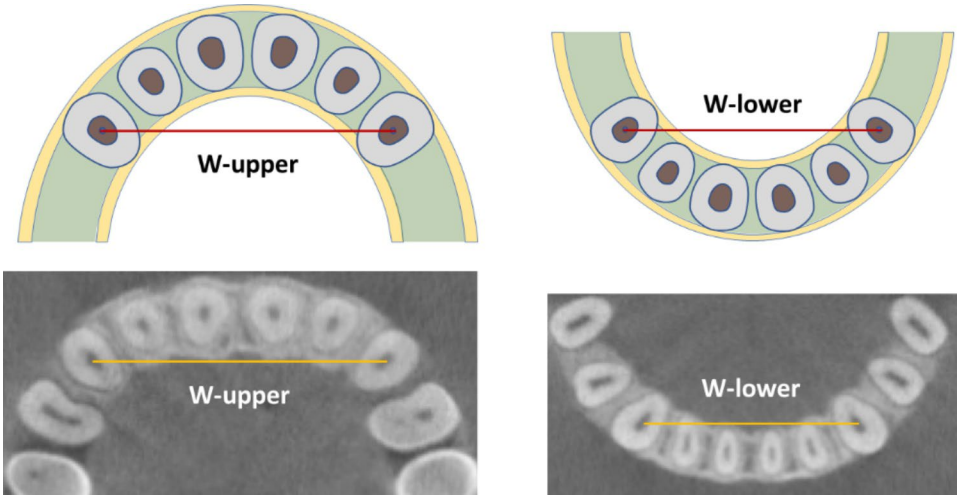

Fig. 6 Maxillary and mandibular inter-cuspid alveolar bone width. W-upper: the maxillary inter-cuspid alveolar bone width; W-lower: the mandibular inter-cuspid alveolar bone width

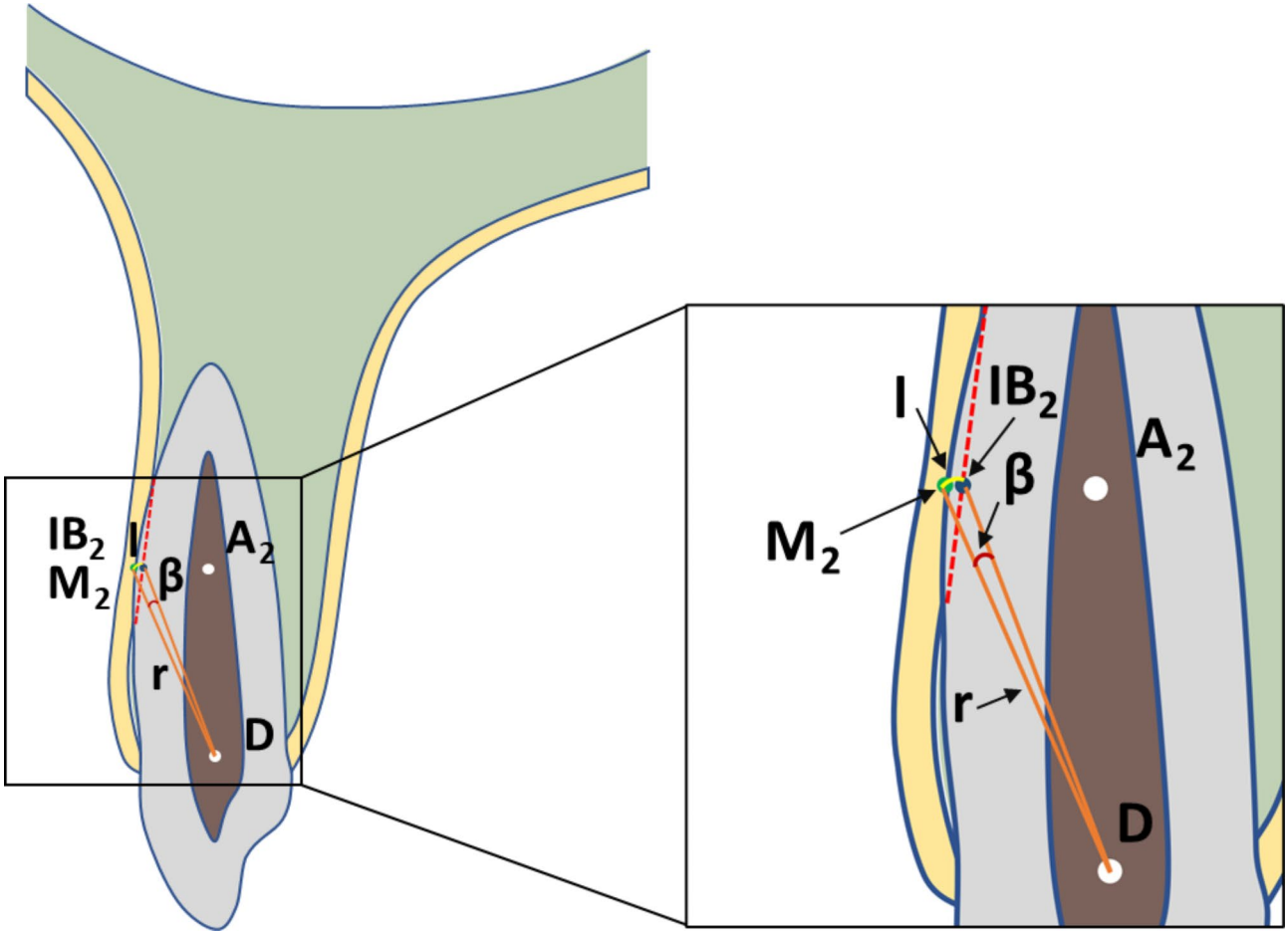

Fig. 7 Ideal root control angle of maxillary cuspids to keep the roots detached from the labial bone cortex. β: the ideal root control angle; $r = M_2\text{-}D = ((A_2\text{-}D)^2 + (A_2\text{-}M_2)^2)^{½}$; $l = 2\pi r \times \beta/360 \approx M_2\text{-}IB_2$; and $\beta \approx (M_2\text{-}IB_2) \times 360 / 2\pi r$

Table 2 Landmarks and definitions based on two-dimensional coordinates

Landmarks		Definitions
Level		
	L_1	The apical root level of the cuspid
	L_2	The mid root level of the cuspid
	L_3	The cervical root level of the cuspid
Root		
	A_1	The apical point of the cuspid
	A_2	The mid root point of the cuspid
	A_3	The 4 mm point below the CEJ of the cuspid
	D	The intersection of the long axis of the cuspid and the CEJ
	M_2	The labial tangent point of the root at the L_2 level
	N_2	The palatal tangent point of the root at the L_2 level
	M_3	The labial tangent point of the root at the L_3 level
	N_3	The palatal tangent point of the root at the L_3 level
Alveolar		
	Q_1	The alveolar bone midpoint of the L_1 section
	Q_3	The alveolar bone midpoint of the L_3 section
	OB_1	The outer edge of the labial bone cortex at the L_1 level
	OB_2	The outer edge of the labial bone cortex at the L_2 level
	OB_3	The outer edge of the labial bone cortex at the L_3 level
	IB_1	The inner edge of the labial bone cortex at the L_1 level
	IB_2	The inner edge of the labial bone cortex at the L_2 level
	IB_3	The inner edge of the labial bone cortex at the L_3 level
	OP_1	The outer edge of the palatal bone cortex at the L_1 level
	OP_2	The outer edge of the palatal bone cortex at the L_2 level
	OP_3	The outer edge of the palatal bone cortex at the L_3 level
	IP_1	The inner edge of the palatal bone cortex at the L_1 level
	IP_2	The inner edge of the palatal bone cortex at the L_2 level
	IP_3	The inner edge of the palatal bone cortex at the L_3 level

Table 3 Measured variables between the alveolar bone and dental landmarks

Abbreviation	Definition
A_1-OB_1	The distance between A_1 to OB_1
A_1-IB_1	The distance between A_1 to IB_1
A_1-OP_1	The distance between A_1 to OP_1
A_1-IP_1	The distance between A_1 to IP_1
A_2-M_2	The distance between A_2 to M_2
A_2-IB_2	The distance between A_2 to IB_2
A_2-OB_2	The distance between A_2 to OB_2
A_2-N_2	The distance between A_2 to N_2
A_2-IP_2	The distance between A_2 to IP_2
A_2-OP_2	The distance between A_2 to OP_2
A_3-M_3	The distance between A_3 to M_3
A_3-IB_3	The distance between A_3 to IB_3
A_3-OB_3	The distance between A_3 to OB_3
A_3-N_3	The distance between A_3 to N_3
A_3-IP_3	The distance between A_3 to IP_3
A_3-OP_3	The distance between A_3 to OP_3
OB_1-OP_1	The apical root alveolar bone thickness
OB_1-IB_1	The apical root labial bone cortical thickness
OP_1-IP_1	The apical root palatal bone cortical thickness
OB_2-OP_2	The mid root alveolar bone thickness
OB_2-IB_2	The mid root labial bone cortical thickness
OP_2-IP_2	The mid root palatal bone cortical thickness
OB_3-OP_3	The cervical root alveolar bone thickness
OB_3-IB_3	The cervical root labial bone cortical thickness
OP_3-IP_3	The cervical root palatal bone cortical thickness
α	The cuspid inclination angle
r	The radius of rotation
β	The rotation angle of the cuspid detached from the labial bone cortex with D as the center of rotation
W-upper	The maxillary intercuspid alveolar bone width
W-lower	The mandibular intercuspid alveolar bone width
WUL	The distance between W-upper and W-lower

sagittal directions, were stable significant variables in A_1-IB_1, M_2-IB_2, and M_3-IB_3.

Discussion

In our study, no differences were found in the alveolar bone thickness, labial bone cortical thickness, and lingual bone cortical thickness in the cuspid region of patients with skeletal class I, II, and III malocclusions. This indicates that the sagittal skeletal discrepancy did not significantly affect alveolar bone thickness in normodivergent facial patterns at different cuspid levels. The mean labial cortical thickness in cuspids ranged from 1.16 to 1.98 mm, similar to the findings of Shen et al., who found that the labial cortical distance of the maxillary cuspids ranged from 0.5 to 1.5 mm [19]. At the middle and cervical root levels, the thickness of the lingual bone cortex was more significant than that of the labial bone cortex, which was consistent with the findings of Lee et al. and Januario et al. [20, 21].

Compared to the labial bone cortex, lingual fenestration and dehiscence rarely occur in anterior teeth [22]. In our study, cuspids of all skeletal classes were in close proximity to the labial bone plate, which makes the cuspids very sensitive to fenestration and dehiscence caused by improper directions of tooth movement. Fenestration and dehiscence in the cuspid region may be associated with thinner buccal bone plates, pressure during the

Table 4 Comparison of the alveolar bone and bone cortical thickness in different skeletal facial patterns

		Class I	Class II	Class III	P
Variables		**Mean ± SD**	**Mean ± SD**	**Mean ± SD**	**value**
L_1 level					
OB_1-OP_1	Men	10.74 ± 1.92	11.43 ± 2.51	11.21 ± 2.26	0.447
	Women	11.49 ± 2.49	10.85 ± 2.66	11.36 ± 1.80	0.475
OB_1-IB_1	Men	1.49 ± 0.29	1.62 ± 0.31	1.56 ± 0.32	0.215
	Women	1.52 ± 0.36	1.66 ± 0.32	1.58 ± 0.37	0.209
OP_1-IP_1	Men	1.39 ± 0.52	1.46 ± 0.55	1.44 ± 0.59	0.782
	Women	1.43 ± 0.72	1.54 ± 0.66	1.36 ± 0.50	0.478
L_2 level					
OB_2-OP_2	Men	9.61 ± 1.34	9.63 ± 1.39	9.82 ± 1.72	0.815
	Women	9.88 ± 0.97	9.38 ± 11.68	9.86 ± 1.73	0.277
OB_2-IB_2	Men	1.04 ± 0.40	1.02 ± 0.36	1.15 ± 0.60	0.468
	Women	1.09 ± 0.58	1.01 ± 0.36	1.10 ± 0.66	0.730
OP_2-IP_2	Men	1.83 ± 0.54	1.73 ± 0.54	1.76 ± 0.43	0.686
	Women	1.86 ± 0.43	1.73 ± 0.65	1.83 ± 0.48	0.554
L_3 level					
OB_3-OP_3	Men	7.73 ± 1.40	7.71 ± 1.21	7.77 ± 1.79	0.985
	Women	7.39 ± 1.45	7.83 ± 1.28	7.95 ± 1.67	0.269
OB_3-IB_3	Men	1.02 ± 0.33	1.03 ± 0.34	1.03 ± 0.36	0.991
	Women	0.97 ± 0.31	1.01 ± 0.33	1.11 ± 0.37	0.248
OP_3-IP_3	Men	1.39 ± 0.45	1.41 ± 0.42	1.26 ± 0.46	0.301
	Women	1.29 ± 0.36	1.27 ± 0.26	1.32 ± 0.48	0.822

*P is significant at 0.05.

†P is significant at 0.01.

SD, standard deviation.

Table 5 Position of the cuspid roots in relation to the alveolar bone in different skeletal facial patterns

		Class I	Class II	Class III	P
Variables		**Mean ± SD**	**Mean ± SD**	**Mean ± SD**	**value**
L_1 level					
A_1-IB_1	Men	0.63 ± 0.83	0.04 ± 0.76	1.10 ± 0.90	<0.001†
	Women	0.93 ± 1.04	−0.11 ± 0.77	0.77 ± 0.79	<0.001†
A_1-OB_1	Men	2.12 ± 0.88	1.66 ± 0.81	2.66 ± 0.92	<0.001†
	Women	2.45 ± 1.23	1.77 ± 0.77	2.35 ± 0.81	0.005†
A_1-IP_1	Men	7.25 ± 1.65	8.31 ± 2.57	7.11 ± 2.32	0.050
	Women	7.61 ± 2.18	7.53 ± 2.59	7.65 ± 2.03	0.977
A_1-OP_1	Men	8.63 ± 1.83	9.77 ± 2.65	8.54 ± 2.12	0.039*
	Women	9.03 ± 2.37	9.07 ± 2.79	9.01 ± 1.90	0.994
L_2 level					
M_2-IB_2	Men	−0.92 ± 0.59	−0.77 ± 0.58	−1.06 ± 0.82	0.188
	Women	−1.07 ± 0.59	−0.81 ± 0.58	−0.88 ± 0.84	0.252
M_2-OB_2	Men	0.12 ± 0.66	0.26 ± 0.70	0.09 ± 0.83	0.597
	Women	0.02 ± 0.63	0.20 ± 0.59	0.22 ± 1.02	0.524
N_2-IP_2	Men	1.58 ± 0.97	1.41 ± 1.09	1.45 ± 1.06	0.779
	Women	1.75 ± 0.84	1.30 ± 0.99	1.35 ± 1.02	0.120
N_2-OP_2	Men	3.42 ± 1.18	3.14 ± 1.10	3.21 ± 1.24	0.604
	Women	3.61 ± 1.02	3.04 ± 1.22	3.19 ± 1.15	0.103
L_3 level					
M_3-IB_3	Men	−0.16 ± 0.62	−0.25 ± 0.50	−0.34 ± 0.73	0.506
	Women	−0.31 ± 0.58	−0.17 ± 0.52	−0.29 ± 0.76	0.543
M_3-OB_3	Men	0.87 ± 0.64	0.78 ± 0.51	0.69 ± 0.67	0.497
	Women	0.66 ± 0.64	0.84 ± 0.48	0.82 ± 0.70	0.410
N_3-IP_3	Men	0.23 ± 0.59	0.13 ± 0.82	0.24 ± 0.60	0.750
	Women	0.47 ± 0.58	0.18 ± 0.60	0.17 ± 0.59	0.065
N_3-OP_3	Men	1.62 ± 0.70	1.54 ± 0.81	1.50 ± 0.77	0.795
	Women	1.76 ± 0.66	1.44 ± 0.65	1.50 ± 0.74	0.127

*P is significant at 0.05.

†P is significant at 0.01.

SD, standard deviation.

masticatory cycle, and a history of previous orthodontic treatment with nonphysiological tooth movement, excessive orthodontic forces, and compromised periodontal tissue integrity [23–26]. Characterization of the position of the cuspids relative to the alveolar bone helps reduce the risk of dehiscence and fenestration [27]. The root of the cuspids closer to the labial cortex indicated that cuspids were physiologically close to the labial bone plate, which may be closely related to the function of cuspids in tearing and cutting food and supporting the corners of the mouth [28]. At the apical root level, the mean A_1-IB_1 was the smallest and even negative in women with skeletal class II malocclusion, indicating that the apical roots of some class II cuspids were located outside the cancellous bone. This suggests that it is hazardous to apply a positive torque to the cuspid roots in skeletal class II malocclusion as it may lead to fenestration in the apical region. At the cervical root level, the roots of teeth

Table 6 Comparison of the distance between the roots of cuspids and the inner and outer edge of labial bone cortex at the different root levels

		L_1 level: A_1-IB_1	L_2 level: M_2-IB_2	L_3 level: M_3-IB_3	P value	P value		
		Mean ± SD	**Mean ± SD**	**Mean ± SD**		**L_1 VS L_2**	**L_2 VS L_3**	**L_1VS L_3**
Class I	Men	0.63 ± 0.83	−0.92 ± 0.59	−0.16 ± 0.62	<0.001†	<0.001†	<0.001†	<0.001†
	Women	0.93 ± 1.04	−1.06 ± 0.59	−0.31 ± 0.58	<0.001†	<0.001†	<0.001†	<0.001†
Class II	Men	0.04 ± 0.76	−0.77 ± 0.58	−0.25 ± 0.50	<0.001†	<0.001†	<0.001†	0.044*
	Women	0.11 ± 0.77	−0.81 ± 0.58	−0.17 ± 0.52	<0.001†	<0.001†	<0.001†	0.054
Class III	Men	1.10 ± 0.90	−1.06 ± 0.82	−0.34 ± 0.73	<0.001†	<0.001†	<0.001†	<0.001†
	Women	0.77 ± 0.79	−0.88 ± 0.84	−0.29 ± 0.76	<0.001†	<0.001†	0.004†	<0.001†

*P is significant at 0.05.

†P is significant at 0.01.

SD, standard deviation.

Table 7 Ideal root control angle to keep the roots of the maxillary cuspids detached from the labial bonebone cortex

		Class I	Class II	Class III	total		P value
Variables		**Mean ± SD**	**Mean ± SD**	**Mean ± SD**	**Mean ± SD**	**n**	
Root length (mm)	Men	15.38 ± 1.61	16.07 ± 2.14	16.03 ± 2.02	15.85 ± 1.96	104	0.275
	Women	15.61 ± 2.30	15.85 ± 2.19	15.70 ± 1.82	15.73 ± 1.82	104	0.787
M_2-IB_2 (mm)	Men	−0.92 ± 0.59	−0.77 ± 0.58	−1.06 ± 0.82	−0.91 ± 0.68	104	0.188
	Women	−1.07 ± 0.59	−0.81 ± 0.58	−0.88 ± 0.84	−0.91 ± 0.68	104	0.252
R (mm)	Men	8.29 ± 0.76	8.64 ± 1.01	8.69 ± 0.85	8.55 ± 0.90	104	0.138
	Women	8.40 ± 1.04	8.54 ± 1.02	8.52 ± 0.81	8.49 ± 0.96	104	0.807
Ideal root control angle (°)	Men	6.32 ± 4.01	5.02 ± 3.78	6.88 ± 5.27	6.03 ± 4.41	104	0.184
	Women	7.26 ± 4.07	5.41 ± 3.70	5.72 ± 5.47	6.08 ± 4.45	104	0.186

*P is significant at 0.05.

†P is significant at 0.01.

SD, standard deviation.

Table 8 Multiple linear regression demonstrating the relationship between cortical anchorage of cuspids and skeletal and dental characteristics

	β	Std. Error	P value
A_1-IB_1			
men			
ANB (°)	−0.072†	0.018	< 0.001
FMA (°)	−0.075*	0.033	0.026
α (°)	−0.054†	0.011	< 0.001
women			
ANB (°)	−0.134†	0.027	< 0.001
FMA (°)	0.100*	0.040	0.014
W-lower (mm)	−0.095*	0.048	0.048
WUL (mm)	0.127†	0.047	0.008
α (°)	−0.073†	0.011	< 0.001
M_2-IB_2			
men			
U_1-SN (°)	−0.025†	0.007	0.001
women			
α (°)	0.021*	0.009	0.028
M_3-IB_3			
men			
FMA (°)	0.083†	0.027	0.003
women			
α (°)	0.021*	0.009	0.028

*P is significant at 0.05.

†P is significant at 0.01.

Std. Error, standard error.

contacted the labial bone cortex in all skeletal malocclusion types and were at risk of bone dehiscence if the cuspids were moving labially. Consistent with our study, studies have found an increase in dehiscence around cuspids after orthodontic treatment [29].

In skeletal class II malocclusion with a deep overbite, we generally first protrude the maxillary and mandibular incisors and then intrude them to avoid anterior alveolar fenestration and dehiscence. The cuspids are positioned close to the incisors and both are often intruded and moved distally at the same time. Therefore, we envisioned the possibility of investigating root control angles of the cuspids to achieve programmed movement similar to that of the incisors. Our study showed that in all skeletal malocclusion groups, the middle part of the root was mostly located in the labial bone cortex. Owing to the large variability in surface morphology and crown length, such as susceptibility to abrasion, the clinical crown center was not chosen, and the midpoint of the CEJ was considered the reference point. As a result, the estimated lingual torque applied was 6.03±4.41° in men and 6.08±4.45° in women. Unfortunately, the large variance reflects an insufficient sample size and within-sample heterogeneity, resulting in limited guidance for clinicians; however, the results suggest that at least positive labial torque should be prudently applied to cuspid roots in general. The importance of careful imaging or oral examination to avoid incorrect treatment on cuspids cannot be ignored.

Cuspid compensation complied with skeletal discrepancy. A recent meta-analysis showed that the relationship between alveolar bone thickness and age had no specific pattern; therefore, age was not considered as a crucial assessment factor in this study and was balanced at baseline [30]. In our study, ANB angle and α were negatively correlated with A_1-IB_1. Therefore, in patients with a large ANB angle or α, it is important to be aware of the risk of fenestration in the apical region of the cuspid. The effect of FMA on cortical anchorage in cuspids was not clear, suggesting that it may be affected by sagittal skeletal malalignment. M_2-IB_2, M_3-IB_3 had fewer influencing factors than A_1-IB_1, probably due to the significant narrowing of the root width of the cuspid from the middle to the apical part of the root, resulting in a greater sensitivity of A_1-IB_1 to skeletal and dental changes.

Characterization of the position of the cuspids relative to the alveolar bone also helps improve orthodontic efficiency [27]. In clear aligner treatment, in addition to the anatomical limitations, poor torque and step settings

can also lower its efficiency in inducing cuspid movements (from 20 to 40%) [31]. In the staging design of invisible orthodontics, it may be advisable to adjust the root position of the cuspids in cancellous bone before intruding them or moving them distally, such as moving the root lingually first. In fixed orthodontics, the inappropriateness of the bracket preset torque and inaccuracy of bracket bonding would affect the achievement of the ideal torque of the cuspids [32]. The currently used MBT, ROTH, and edgewise straight wire arch orthodontic systems have preset torques of −2°, −7°, and 0° for cuspids, respectively. According to our findings, preset negative torque on cuspids in their original position could lead to cortical anchorage of the cuspids, and subsequently, adversely affect the adjacent teeth, lead to stagnation, or induce root resorption during orthodontic treatment.

Our study has some limitations. First, for the same inner skeletal pattern, our study did not reveal whether arch form affected the position of the cuspids. Second, the observations in the three defined planes cannot truly depict the relationship between the root morphology of cuspids and the bone cortex. The portion of cuspids located within the bone cortex may lie between the three levels. The determination of this level depends on improving CBCT accuracy, advancement of image recognition technology, optimization of intuitive artificial intelligence fixed-point curve fitting, and accumulation of data volume. Moreover, we included only normodivergent patients with well aligned cuspid, and the generalized application of the findings is limited. Imaging or oral examination, considerations of biology and biomechanics, and flexible therapeutic strategies are always kept pace with patient's individual characteristics. Further studies including large samples focusing on cuspid morphology, periodontal condition, and different skeletal patterns are needed to explore the relationship between cuspids and alveolar bone.

Conclusions

Our study demonstrated the characteristics of cuspid roots cortical anchorage and the factors influence the relationship between cuspid root and alveolar bone cortex in different sagittal skeletal patterns using 3D images, which provides a reference for clinicians to better implement orthodontic treatment and reduce complications. Importantly, 6.03±4.41° (male) and 6.08±4.45° (female) may be the appropriate root control angles to keep the roots of maxillary cuspids detached from the labial bone cortex. However, we only focused on normodivergent patients. Future studies on cuspids including large samples with different skeletal patterns are needed to enhance clinical treatment.

List of Abbreviations

CBCT cone-beam computed tomography
CEJ cemento-enamel junction
FMA Frankfort mandibular plane angle

Acknowledgements
Not applicable.

Author Contribution
XW designed the study. XW, YL, GZ, LZ and JZ collected data. XW, YL and GZ performed data analysis. XW and YY prepared the manuscript; QZ revised and proofread the manuscript. All authors approved the final manuscript.

Funding
This study was supported by the National Natural Science Foundation of China (Grant nos. 82171003 and 81870745).

Data Availability
The datasets generated and analyzed during the current study are not publicly available due to individual privacy but are available from the corresponding author on reasonable request.

Declarations

Ethics approval and consent to participate
This retrospective cross-sectional study was approved by the Ethics Committee of the National Key Laboratory of Oral Diseases and the Ethics Committee of the West China Stomatology Hospital of Sichuan University (protocol number: WCHSIRB-D-2020-399). All methods were performed in accordance with the relevant guidelines and regulations. Informed consent was obtained from all individual participants involved in the study.

Consent for publication
Not applicable.

Competing interests
The authors declared no competing interests.

Received: 6 November 2022 / Accepted: 26 March 2023
Published online: 15 April 2023

References

1. Hennessy J, Al-Awadhi EA. Clear aligners generations and orthodontic tooth movement. J Orthod. 2016;43(1):68–76.
2. McLaughlin RP, Bennett JC. Evolution of treatment mechanics and contemporary appliance design in orthodontics: a 40-year perspective. Am J Orthod Dentofacial Orthop. 2015;147(6):654–62.
3. Hösl E, Baldauf A. Mechanical and biological basics in orthodontic therapy. Medicine. 1991.
4. Uzuner FD, Yücel E, Göfteci B, Gülsen A. The effect of corticotomy on tooth movements during canine retraction. J Orthod Res. 2015;3(3):181.
5. Ghafari JG, Ammoury MJ. Overcoming compact bone resistance to tooth movement. Am J Orthod Dentofacial Orthop. 2020 Sep;158(3):343–8.
6. AlAli F, Atieh MA, Hannawi H, Jamal M, Harbi NA, Alsabeeha NHM, et al. Anterior Maxillary Labial Bone Thickness on Cone Beam Computed Tomography. Int Dent J. 2022. https://doi.org/10.1016/j.identj.2022.03.007
7. Jin S-H, Park J-B, Kim N, Park S, Kim KJ, Kim Y, et al. The thickness of alveolar bone at the maxillary canine and premolar teeth in normal occlusion. J Periodontal Implan. 2012;42(5):173–8.
8. Elnagar MH, Handelman CS, Lippincott JS, Kim MR, BeGole E. Alveolar cortical plate changes associated with incisor retraction and its influence on the limits of orthodontic tooth movement. Orthod Craniofac Res. 2021;24(4):536–42.
9. Kapila S, Conley RS, Harrell WE Jr. The current status of cone beam computed tomography imaging in orthodontics. Dentomaxillofac Radiol. 2011;40(1):24–34.
10. Yagci A, Veli I, Uysal T, Ucar FI, Ozer T, Enhos S. Dehiscence and fenestration in skeletal class I, II, and III malocclusions assessed with cone-beam computed tomography. Angle Orthod. 2012;82(1):67–74.

11. Ma J, Huang J, Jiang J-h. Morphological analysis of the alveolar bone of the anterior teeth in severe high-angle skeletal class II and Class III malocclusions assessed with cone-beam computed tomography. PLoS ONE. 2019;14(3):e0210461.
12. Lu C-L, Li B-W, Yang M, Wang X-Q. Relationship between alveolar-bone morphology at the mandibular incisors and their inclination in adults with low-angle, skeletal class III malocclusion—A retrospective CBCT study. PLoS ONE. 2022;17(3):e0264788.
13. Coşkun İ, Kaya B. Appraisal of the relationship between tooth inclination, dehiscence, fenestration, and sagittal skeletal pattern with cone beam computed tomography. Angle Orthod. 2019;89(4):544–51.
14. Park M-S, Park Y-B, Choi H, Moon H-S, Chung M-K, Cha I-H, et al. Morphometric analysis of maxillary alveolar regions for immediate implantation. J Adv Prosthodont. 2013;5(4):494–501.
15. De Vos W, Casselman J, Swennen GRJ. Cone-beam computerized tomography (CBCT) imaging of the oral and maxillofacial region: a systematic review of the literature. Int J Oral Maxillofac Implants. 2009;38(6):609–25.
16. Leung CC, Palomo L, Griffith R, Hans MG. Accuracy and reliability of cone-beam computed tomography for measuring alveolar bone height and detecting bony dehiscences and fenestrations. Am J Orthod Dentofacial Orthop. 2010;137(4):109–S19.
17. Hu X, Huang X, Gu Y. Assessment of buccal and lingual alveolar bone thickness and buccolingual inclination of maxillary posterior teeth in patients with severe skeletal class III malocclusion with mandibular asymmetry. Am J Orthod Dentofacial Orthop. 2020;157(4):503–15.
18. Sun L, Zhang L, Shen G, Wang B, Fang B. Accuracy of cone-beam computed tomography in detecting alveolar bone dehiscences and fenestrations. Am J Orthod Dentofacial Orthop. 2015;147(3):313–23.
19. Shen JW, He FM, Jiang QH, Shan HQ. Measurement of facial bone wall thickness of maxillary anterior teeth and premolars on cone beam computed tomography images. Zhejiang Da Xue Xue Bao Yi Xue Ban. 2012;41(3):234–8.
20. Lee S-L, Kim H-J, Son M-K, Chung C-H. Anthropometric analysis of maxillary anterior buccal bone of korean adults using cone-beam CT. J Adv Prosthodont. 2010;2(3):92–6.
21. Januário AL, Duarte WR, Barriviera M, Mesti JC, Araújo MG, Lindhe J. Dimension of the facial bone wall in the anterior maxilla: a cone-beam computed tomography study. Clin Oral Implants Res. 2011;22(10):1168–71.
22. Kim Y, Park JU, Kook YA. Alveolar bone loss around incisors in surgical skeletal class III patients. Angle Orthod. 2009;79(4):676–82.
23. Evangelista K, Vasconcelos Kde F, Bumann A, Hirsch E, Nitka M, Silva MA. Dehiscence and fenestration in patients with class I and Class II Division 1 malocclusion assessed with cone-beam computed tomography. Am J Orthod Dentofacial Orthop. 2010;138(2):133. .e1-7; discussion – 5.
24. Enhos S, Uysal T, Yagci A, Veli İ, Ucar FI, Ozer T. Dehiscence and fenestration in patients with different vertical growth patterns assessed with cone-beam computed tomography. Angle Orthod. 2012;82(5):868–74.
25. Abdelmalek RG, Bissada NF. Incidence and distribution of alveolar bony dehiscence and fenestration in dry human egyptian jaws. J Periodontol. 1973;44(9):586–8.
26. Fuhrmann R. Three-dimensional interpretation of periodontal lesions and remodeling during orthodontic treatment. Part III. J Orofac Orthop. 1996;57(4):224–37.
27. Antoun JS, Mei L, Gibbs K, Farella M. Effect of orthodontic treatment on the periodontal tissues. Periodontol 2000. 2017;74(1):140–57.
28. McGee GF. Tooth placement and base contour in denture construction. J Prosthet Dent. 1960;10(4):651–7.
29. Alvarez MA, Mejia A, Alzate D, Rey D, Ioshida M, Aristizabal JF, et al. Buccal bone defects and transversal tooth movement of mandibular lateral segments in patients after orthodontic treatment with and without piezocision: a case-control retrospective study. Am J Orthod Dentofacial Orthop. 2021;159(3):e233–e43.
30. Shafizadeh M, Tehranchi A, Shirvani A, Motamedian SR. Alveolar bone thickness overlying healthy maxillary and mandibular teeth: a systematic review and meta-analysis. Int Orthod. 2021;19(3):389–405.
31. Rossini G, Parrini S, Castroflorio T, Deregibus A, Debernardi CL. Efficacy of clear aligners in controlling orthodontic tooth movement: a systematic review. Angle Orthod. 2015;85(5):881–9.
32. Sondhi A. The implications of bracket selection and bracket placement on finishing details. Semin Orthod. 2003;9:155–64.

Publisher's Note

Springer Nature remains neutral with regard to jurisdictional claims in published maps and institutional affiliations.